Acta Crystallographica Section F
Structural Biology and Crystallization Communications
ISSN 1744-3091

Crystallization and preliminary X-ray studies of dUTPase from Mason–Pfizer monkey retrovirus

Orsolya Barabás,‡ Veronika Németh‡ and Beáta G. Vértessy*

Institute of Enzymology, BRC, Hungarian Academy of Sciences, Budapest, Karolina út 29, H-1113, Hungary

‡ These authors contributed equally to this work.

Correspondence e-mail: vertessy@enzim.hu

Received 22 December 2005
Accepted 9 March 2006

Deoxyuridine 5′-triphosphate nucleotidohydrolase from Mason–Pfizer monkey retrovirus (M-PMV dUTPase) is a betaretroviral member of the dUTPase enzyme family. In the mature M-PMV virion, this enzyme is present as the C-terminal domain of the fusion protein nucleocapsid-dUTPase. The homotrimeric organization characteristic of dUTPases is retained in this bifunctional fusion protein. The fusion protein supposedly plays a role in adequate localization of dUTPase activity in the vicinity of nucleic acids during reverse transcription and integration. Here, the nucleocapsid-free dUTPase (48 426 Da) was cocrystallized with a dUTP substrate analogue using the hanging-drop vapour-diffusion method. The obtained crystals belong to the primitive hexagonal space group $P6_3$, with unit-cell parameters a = 60.6, b = 60.6, c = 63.6 Å, α = 90, β = 90, γ = 120°. Native and $PtCl_4$-derivative data sets were collected using synchrotron radiation to 1.75 and 2.3 Å, respectively. Phasing was successfully performed by isomorphous replacement combined with anomalous scattering.

1. Introduction

dUTPases are responsible for regulating cellular dUTP:dTTP ratios by catalyzing the hydrolysis of dUTP into the dTTP precursor dUMP and pyrophosphate. Lack of enzymatic activity leads to high levels of incorporation of deoxyuridine moieties into DNA. Uracil-DNA transforms base-excision repair into a hyperactive futile cycle resulting in thymine-less cell death by chromosome fragmentation (Pearl & Savva, 1996; Goulian *et al.*, 1986). All free-living organisms, as well as several DNA and retroviruses, encode dUTPase. The enzyme is essential for viability in prokaryotes and eukaryotes and contributes to the host-range preferences and infectivity of viruses (el-Hajj *et al.*, 1988; Lerner *et al.*, 1995; Turelli *et al.*, 1997).

Betaretroviral genomes contain the dUTPase gene adjacent to the gene for the nucleocapsid polypeptide. Virion lysates show dUTPase activity, indicating enzyme encapsulation in the virion. In the betaretroviruses mouse mammary tumour virus (MMTV) and Mason–Pfizer monkey virus (M-PMV), two ribosomal frameshifts between *gag* and *pro* and *pro* and *pol* frames occur, yielding Gag-Pro and Gag-Pro-Pol polyproteins. The first frameshift gives rise to a transframe fusion protein joining the nucleocapsid (NC) and dUTPase polypeptides (NC-dUTPase). Recently, NC-dUTPase was shown to be present in a stable form resisting proteolysis by retroviral and cellular proteases in the M-PMV virion as well as in M-PMV virus-infected cells (Barabas *et al.*, 2003). The fusion protein is the only physiological form of M-PMV dUTPase. M-PMV NC-dUTPase retains both nucleic acid-binding and dUTP-hydrolyzing catalytic activity (Barabas *et al.*, 2003).

The nucleocapsid (NC) protein plays an essential role in retroviral assembly, genomic RNA encapsidation, reverse transcription and integration. NC protein is rich in basic amino acids and contains two Zn-knuckle structural motifs that coordinate zinc ions and participate in nucleic acid recognition (Gao *et al.*, 1998). While both the enzymatic function of dUTPase and the multiple functions of NC protein have been studied in detail, the exact role of NC-dUTPase in the virus life cycle has not yet been clarified. The catalytic rate constant of recombinant M-PMV NC-dUTPase was shown to be decreased tenfold compared with other retoviral, bacterial or eukaryotic

dUTPases (Barabas *et al.*, 2003). The structural background responsible for the low catalytic efficiency may be identified by high-resolution three-dimensional structural analysis. In this paper, we describe the crystallization and structure-determination process of M-PMV NC-dUTPase in complex with a dUTP substrate analogue.

2. Materials and methods

2.1. Expression and purification

Expression and purification of M-PMV NC-dUTPase was based on previously described protocols (Barabas *et al.*, 2003). In order to optimize crystallization, the following alterations were introduced. BL21(DE3) *Escherichia coli* cells transformed with the expression plasmid were propagated to an OD_{600} of 0.4 and then induced by addition of isopropyl β-D-thiogalactoside to a final concentration of 1 m*M*. Cells were harvested after 4 h incubation at 310 K. All the following procedures were performed on ice or in a cold room (at 273–280 K). Cell pellets were solubilized in 1/10 volume of lysis buffer [50 m*M* Tris–HCl pH 8.5 containing 150 m*M* NaCl, 1 m*M* EDTA, 5 m*M* dithiothreitol (DTT), 0.5 m*M* phenylmethanesulfonyl fluoride (PMSF) and 2 µg ml^{-1} each of RNase and DNase]. Cell suspensions were stirred for 30 min, sonicated (3–5 × 60 s), stirred again for 20 min and centrifuged (12 000*g* for 30 min). Supernatants were directly loaded onto a HiTrap Heparin HP column (5 ml), equilibrated in 50 m*M* Tris buffer pH 8.0 containing 150 m*M* NaCl, 5 m*M* DTT and 0.1 m*M* PMSF and developed using 200 ml of a linear gradient to 1 *M* NaCl. NC-dUTPase appeared at 0.35–0.5 *M* NaCl. Gel filtration was carried out on a Superdex 200 HR column in 50 m*M* Tris–HCl buffer pH 8.0 containing 500 m*M* NaCl, 5 m*M* DTT and 0.1 m*M* PMSF. Purification was completed in less than 30 h following cell lysis. The catalytic activity of the prepared protein samples was ascertained by continuous spectrophotometric assay as described in Barabas *et al.* (2003).

2.2. Crystallization

The purified protein was dialyzed against 50 m*M* Tris–HCl buffer pH 8.0 containing 200 m*M* NH_4Cl, 5 m*M* DTT and 0.5 m*M* PMSF and concentrated to 5–7 mg ml^{-1} using centrifugal concentrator devices (Millipore). Crystals were grown at room temperature by hanging-drop vapour diffusion in VDX hanging-drop plates (Hampton Research). Preliminary crystallization experiments were carried out with Crystal Screen reagent kits I and II (Hampton Research). The protein solution prepared for crystallization contained 5 mg ml^{-1} enzyme, 1.3 m*M* α,β-imino-dUTP substrate analogue and 10 m*M* $MgCl_2$ in 50 m*M* Tris–HCl buffer pH 8.0 and 200 m*M* NH_4Cl. The dUTPase/α,β-imino-dUTP/Mg^{2+} solution was mixed with reservoir solution in a 1:1 ratio in 2 µl drops. The volume of the reservoir solution was 1 ml.

Figure 1
NC-dUTPase crystals (with maximum dimensions of ∼0.5 × 0.15 × 0.15 mm) grown in 0.1 *M* Tris–HCl pH 8.5 and 8%(*w*/*v*) PEG 8000.

2.3. Data collection and processing

For data collection, crystals were cryoprotected by the addition of 8% 2-methyl-2,4-pentanediol and flash-cooled in a 100 K nitrogen-gas stream. Native data were collected at station PX13 at EMBL/DESY, Hamburg, Germany and processed with the programs *DENZO* and *SCALEPACK* (Otwinowski & Minor, 1997). For phasing, a Pt derivative was prepared by soaking a crystal overnight in reservoir solution containing 10 m*M* K_2PtCl_4. A single data set was collected at the Pt peak energy at ID14-4 at ESRF, Grenoble, France and data were processed using *MOSFLM* and *SCALA* (Leslie, 1992; Evans, 1997).

2.4. Initial structure determination

The structure was solved by experimental phasing with two platinum sites based on isomorphous and anomalous differences (SIRAS) of this derivative using the *SOLVE*/*RESOLVE* package (Terwilliger & Berendzen, 1999).

3. Results and discussion

The purity of the final protein preparation was greater than 95% by SDS–PAGE analysis. The conformational homogeneity of the sample was checked by dynamic light scattering (DLS) as described in Barabas *et al.* (2003), providing polydispersity values of less than 20% for each protein sample subjected to crystallization. In the preliminary crystallization trials the first crystals appeared after nine months, but further optimization of the crystallization parameters resulted in crystals that grew to final size in less than 3 d. The original conditions were fine-screened for precipitating agent and protein concentration as well as buffer type and pH. The best quality crystals were obtained after microseeding from a condition containing 0.1 *M* Tris–HCl buffer pH 8.5 and 8%(*w*/*v*) PEG 8000 in the well solution. The PEG 8000 stock solution was 40%(*w*/*v*). These crystals reached final dimensions of about 0.5 × 0.15 × 0.15 mm (Fig. 1). The catalytic competence of the enzyme in the crystal phase was shown by competition experiments with the native substrate dUTP on washed crystals. Hydrolysis was followed by a discontinuous thin-layer chromatography activity test (Barabas *et al.*, 2003). According to analysis of dissolved crystals by mass spectrometry and gel electrophoresis, the NC segment is lacking from the crystallized protein (probably as a consequence of proteolytic degradation) and therefore the crystals only contained the 150 residues that form the dUTPase domain. [The mass-spectrometric analysis was performed at the Interdisciplinary Clinical Research Center (IZKF) for Integrated Functional Genomics, University of Münster, Germany.]

The optimized crystals allowed the collection of a complete data set to 1.75 Å using synchrotron radiation. The NC-free dUTPase protein formed primitive hexagonal crystals which belong to space group $P6_3$. The unit cell (202 270.7 Å^3) can accommodate 3–7 molecules of the 16 142 Da molecular-weight protein with reasonable packing density. Provided that the $P6_3$ space group contains six asymmetric units, assuming one protein chain (one monomer) per asymmetric unit, the unit-cell content analysis results in a Matthews coefficient of 2.08 Å^3 Da^{-1} and a solvent content of 43.83%.

Structure-solution trials using molecular replacement failed with all dUTPase model molecules available from the PDB. In order to

Table 1
Data-collection, processing and phasing statistics.

Values in parentheses are for the highest resolution shell.

	Native complex	$PtCl_4^{2-}$ derivative
Ligands bound	α,β-Imino-dUTP, Mg^{2+}	α,β-Imino-dUTP, Mg^{2+}
Space group	$P6_3$	$P6_3$
Unit-cell parameters (Å)	$a = b = 60.6$, $c = 63.6$	$a = b = 60.3$, $c = 63.9$
Wavelength (Å)	0.8028	1.0720
Resolution range (Å)	20.0–1.75 (1.77–1.75)	30.2–2.3 (2.38–2.30)
Measured reflections	153156 (4928)	112416 (7744)
Unique reflections	13423 (438)	5866 (565)
Completeness (%)	99.8 (100)	98.8 (98.8)
$\langle I/\sigma(I)\rangle$	44.8 (4.4)	9.3 (2.3)
R_{sym}† (%)	3.2 (40.2)	6.1 (32.4)
Phasing analysis		
Resolution (Å)		20–2.3
No. of sites		2
Mean figure of merit (FOM)		0.405
Beamline	EMBL/DESY X13	ESRF ID14-4
Detector	MAR CCD	Q315r ADSC CCD

† $R_{sym} = \sum |I - \langle I\rangle| / \sum I$, where I represents the intensity of the reflection and $\langle I\rangle$ the averaged intensity.

obtain experimental phases, several heavy-atom compounds, namely Ba^{2+}, Sr^{2+}, ethylmercury phosphate and further mercury compounds, Au compounds, bromide and iodine, were assessed for the production of good-quality derivatives for phase determination. Derivatization with $PtCl_4^{2-}$ appeared to be the most successful and provided good-quality phases using the SIRAS technique. Data-collection, processing and phasing statistics are given in Table 1. Based on the experimental phases, a good-quality initial map (Fig. 2) was produced that clearly locates densities for the substrate-analogue ligand and the Mg^{2+} cofactor. Further refinement of the structure is in progress.

Support was provided by grants from the Hungarian National Research Foundation (T 034120, TS 044730, M 27852 to BGV), the Howard Hughes Medical Institutes, USA (grant No. 55000342 to BGV), the Alexander von Humboldt Foundation, Germany, the Aventis/Institut de France Scientia Europeae Prize, France (to BGV) and the European Community Marie Curie Training Sites (HPMT-CT-20000-00174 to OB). Drs Iva Pichova and Michaela Rumlova are thanked for the expression plasmids, Katja Schirwitz for helpful suggestions in protein purification, László Sallai for invaluable help in phasing and the beamlines and operators at EMBL/DESY, Hamburg and ID14-4, ESRF, Grenoble for data-collection opportunities.

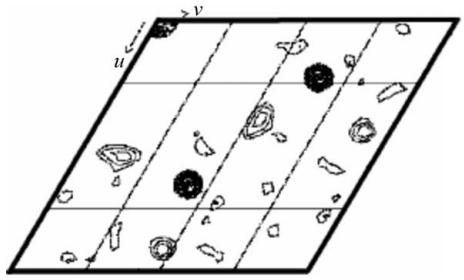

Figure 2
The isomorphous difference Patterson map.

References

Barabás, O., Rumlova, M., Erdei, A., Pongracz, V., Pichova, I. & Vértessy, B. G. (2003). *J. Biol. Chem.* **278**, 38803–38812.
el-Hajj, H. H., Zhang, H. & Weiss, B. (1988). *J. Bacteriol.* **170**, 1069–1075.
Evans, P. R. (1997). *Jnt CCP4/ESF–EACBM Newsl. Protein Crystallogr.* **33**, 22–24.
Gao, Y., Kaluarachchi, K. & Giedroc, D. P. (1998). *Protein Sci.* **7**, 2265–2280.
Goulian, M., Bleile, B. M., Dickey, L. M., Grafstrom, R. H., Ingraham, H. A., Neynaber, S. A., Peterson, M. S. & Tseng, B. Y. (1986). *Adv. Exp. Med. Biol.* **195**, 89–95.
Lerner, D. L., Wagaman, P. C., Phillips, T. R., Prospero-Garcia, O., Henriksen, S. J., Fox, H. S., Bloom, F. E. & Elder, J. H. (1995). *Proc. Natl. Acad. Sci. USA*, **92**, 7480–7484.
Leslie, A. G. W. (1992). *Jnt CCP4/ESF–EACBM Newsl. Protein Crystallogr.* **26**.
Otwinowski, Z. & Minor, W. (1997). *Methods Enzymol.* **276**, 307–326.
Pearl, L. H. & Savva, R. (1996). *Nature Struct. Biol.* **3**, 485–487.
Terwilliger, T. C. & Berendzen, J. (1999). *Acta Cryst.* D**55**, 849–861.
Turelli, P., Guiguen, F., Mornex, J. F., Vigne, R. & Querat, G. (1997). *J. Virol.* **71**, 4522–4530.